Int J Physiol Pathophysiol Pharmacol 2026;18(1):1-7
www.ijppp.org /ISSN:1944-8171/IJPPP0169499

Review Article

A comparative study of artifact reduction techniques in metal-implanted CT scans

Diana Rafieezadeh[1], Amirreza Khalaji[2], Ava Goli[1], Ali Gharavinia[3], Hossein Mohammadi[3]

[1]Department of Cellular and Molecular Biology, Razi University, Kermanshah, Iran; [2]Faculty of Medicine, Tabriz University of Medical Sciences, Tabriz, Iran; [3]School of Medicine, Isfahan University of Medical Sciences, Isfahan, Iran

Received October 23, 2025; Accepted January 28, 2026; Epub February 15, 2026; Published February 28, 2026

Abstract: Over the past few decades, X-ray computed tomography (CT) has been introduced as one of the main cross-sectional imaging methods in a wide range of clinical applications in diagnostic radiology, oncology, and multimodality molecular imaging. Despite the acknowledged value of this imaging method, in some cases, the quality of CT images is affected by the presence of metallic implants. The presence of metal objects such as dental fillings, hip or knee prostheses, pacemakers, war shrapnel, and spinal cages cause and exacerbate image artifacts. These types of artifacts appear in the image as black and white lines that obscure the structures and tissues surrounding the metal implant and destroy the diagnostic value of CT images. These artifacts also affect the accuracy of radiotherapy treatment planning, which relies on CT images to characterize electron density and estimate the relative stopping power of particles. Therefore, to solve this problem, over the past 4 decades, algorithms called Metal Artifact Reduction (MAR) have been proposed. The objective of this study was to assess the five MAR algorithms using simulation and clinical studies. The algorithms include linear interpolation (LI-MAR) of degraded data in sinograms, normalization metal artifact reduction (NMAR), metal removal method (MDT), metal artifact reducer for orthopedic implants (OMAR), and a method based on iteration-based algorithms (MAP). Clinical images in different body regions, with different dimensions and types of metal implants, have been studied to evaluate the performance of MAR algorithms. To quantitatively assess the quality of images modified with MAR algorithms, the normalized root mean square error (NRMSE) criterion has been calculated and evaluated. The results of the algorithm evaluation showed that the NMAR algorithm was more efficient than other algorithms in reducing metal artifacts in most cases. Also, the algorithm processing time parameter demonstrated the clinical value of the NMAR algorithm.

Keywords: Metal artifact reduction (MAR), computed tomography artifacts, CT image quality, interpolation-based MAR

Introduction

Computed tomography (CT) has become an essential imaging modality in modern medicine, offering high-resolution imaging for diagnosis and treatment planning. Despite advances in scanner technology that have improved image quality and reduced imaging time, the presence of metal objects in the field of view remains a major challenge [1]. Metal implants, surgical instruments, or foreign bodies severely attenuate X-rays and cause faulty projections, which ultimately lead to severe artifacts in the reconstructed images [2]. These artifacts usually appear as elongated lines or light and dark bands, reducing diagnostic accuracy and obscuring clinically important structures [3].

Metal artifacts are mainly caused by beam hardening, scattering, and photon noise. These artifacts are especially important in situations such as chest CT imaging of COVID-19 patients, where accurate assessment of lung tissue is essential [4]. Metal implants near the lungs can create star-shaped linear artifacts, which complicates the detection of lesions or tumors and potentially affects dose estimates in radiation therapy planning [5].

To address these challenges, metal artifact reduction (MAR) algorithms have been developed and widely used. It is notable to say that MAR acts in projection space and replace corrupted projections caused by metal with interpolation from neighboring uncorrupted projec-

https://doi.org/10.62347/GFJJ2560

tions [5, 6]. MAR methods are generally divided into two categories: interpolation-based and iteration-based [6]. Interpolation-based methods repair corrupted projections by estimating missing data from neighboring healthy areas, while iteration-based methods improve image reconstruction incrementally to increase accuracy [7]. Commercial implementations, such as the Orthopedic Metal Artifact Reduction (OMAR) system, offer practical solutions for clinical applications. A thorough understanding of these algorithms and their relative strengths is crucial for optimizing the quality of CT images in both research and clinical settings [8].

Methods

In the past four decades, numerous efforts have been made to introduce methods to reduce and eliminate the effects of metal artifacts in CT images. In this context, MAR methods are generally divided into two main categories: 1. Interpolation-based methods; 2. Iteration-based methods.

Most MAR techniques have advantages and disadvantages, including computational simplicity, accuracy, and effectiveness in reducing artifacts caused by a variety of metal objects, as well as the possibility of creating new artifacts. Therefore, the diverse features and potential performance of these algorithms require a comprehensive comparative evaluation to better understand the strengths and weaknesses of each method [9].

In this study, five common MAR methods were investigated-specifically, two interpolation-based sinogram correction methods and three iteration-based methods, which will be explained in the following sections [10].

Interpolation-based methods

These methods are widely used due to their simplicity, ease, and speed of execution of computer programs based on them. In general, such methods consist of two main steps: 1. Identifying metal regions and their corresponding projections in the sinogram matrix. 2. Removing the corrupted projections and replacing them through interpolation from the intact neighboring data.

In most of these methods, the metallic region is identified in the original image using thresholding or other segmentation techniques. The identified metallic region is then transferred into the sinogram domain, and the projections associated with this region are isolated [11]. In other approaches, the projections corresponding to the metallic region are directly separated from the sinogram generated from the original image using segmentation methods. These separated data are treated as missing data [12].

As part of the research background, Kalender and colleagues (1987) proposed a MAR algorithm based on simple linear interpolation. Linear interpolation methods can introduce new artifacts in the reconstructed image, which, in some cases, may be even more severe than those in the original image [6]. The main reason for these artifacts is the improper recovery of corrupted data in the sinogram matrix, due to the discontinuity of interpolated data along the second dimension of the sinogram matrix [13].

Efforts to improve the performance of the simple linear interpolation method by Meter and colleagues led to the development of a new approach. This approach, known as Normalized Metal Artifact Reduction (NMAR), employs so-called background images to enhance the reconstruction of corrupted images. Background images are generated by classifying the image into air, soft tissue, and bone categories [14].

Iteration-based methods

Alongside MAR approaches that use interpolation techniques to correct artifacts, a number of algorithms have been investigated with the aim of correcting corrupted projections through iteration-based methods [15, 16].

Another algorithm classified under iteration-based methods, which has been evaluated in several studies, is known as the Metal Deletion Technique (MDT). This method addresses the limitations of interpolation by applying image filtering, replacing corrupted projections with corrected ones, and repeating this process iteratively [17].

A further iteration-based algorithm, which is a commercially available clinical solution implemented on Philips systems, is known as Orthopedic Metal Artifact Reduction (OMAR). In

the present study, this algorithm was selected and evaluated as an example of an existing commercial method for addressing metal artifacts in CT images, which has been reviewed in multiple studies [18].

In this study, five common metal artifact reduction methods were used, including MDT, OMAR, MAP, NMAR, and LI-MAR. In MDT, sinogram profiles are reconstructed using multidomain modeling and distorted areas are filled in [6]. OMAR attenuates artifacts by identifying metal-induced saturation regions and performing adaptive filtering on the sinogram. MAP uses a posterior maximization framework to estimate the optimal image considering the noise model and metal scattering [8-10]. NMAR first normalizes the original image and then replaces the distorted values with reference projections. In LI-MAR, linear interpolation is performed in the damaged areas of the sinogram and then the final image is reconstructed. These methods were evaluated on both simulated and clinical image sets [14].

Simulation

For the study and evaluation of the performance of the aforementioned methods (MDT, OMAR, MAP, NMAR, LI-MAR), both simulated and clinical images were used. In clinical images, it is impossible to obtain a slice that is simultaneously affected by metal artifacts and, at the same time, available in a metal-free form [19]. To achieve such a condition, a simulation algorithm was employed. In this simulation, a CT image of a patient without metallic implants was acquired, and the CT numbers of each pixel were then converted into the corresponding attenuation coefficients [10]. To simulate projections generated by X-rays passing through multiple metals, the material composition of each pixel must be known. Therefore, a threshold-based weighting method was applied to segment the image into bone and soft tissue (water equivalent) [20].

Findings

All the algorithms under study were implemented in MATLAB based on previously evaluated algorithms reported in the literature. To qualitatively assess the performance of the introduced MAR algorithms, five clinical images from different regions of the body were acquired, encompassing metallic implants of varying sizes and compositions. The clinical images, corrupted by metal artifacts, were processed using the five MAR algorithms. The results of this evaluation are shown in **Figure 1** [21].

Overall, all algorithms introduced some new artifacts in the form of bright and dark streaks in the corrected images. The magnitude of these secondary artifacts varied depending on the type of algorithm and the size and density of the metallic implants. The intensity of secondary artifacts in images corrected with the NMAR algorithm was lower compared to other algorithms. Column 2 corresponds to head coils, where the artifact intensity was relatively low. Consequently, almost all algorithms provided satisfactory correction for this image. In this case, the NMAR and MDT algorithms performed better than the other methods.

The evaluation indices included quantitative measurements of metal-induced distortion, preservation of texture details, and the degree of contrast improvement in areas adjacent to the implant. For quantitative evaluation, metrics such as RMSE, PSNR, and SSIM were calculated between the reference and corrected images. Additionally, for clinical images lacking a metal-free reference, a quality assessment was performed by a radiologist based on artifact reduction, edge clarity, and tissue naturalness. The intensity profile in the paths passing through the metal area was also examined to assess the stability and uniformity of the reconstruction. This set of indicators allowed for a fair comparison of the performance of different MAR methods.

In Column 3, filled teeth produced severe artifacts in the image, due to the high number of fillings and the high density of the restorative materials. Almost none of the algorithms were able to recover the corrupted data in this scenario. A comparative analysis indicates that the NMAR algorithm generally outperformed the other methods. Column 4 corresponds to the pelvis and spinal vertebrae, where the image was heavily corrupted by metallic artifacts. In this case, due to the severity of the artifacts, the MAR algorithms were unable to effectively reduce the metal-induced distortions. Column 5 shows metal artifacts of low intensity, caused by the presence of small

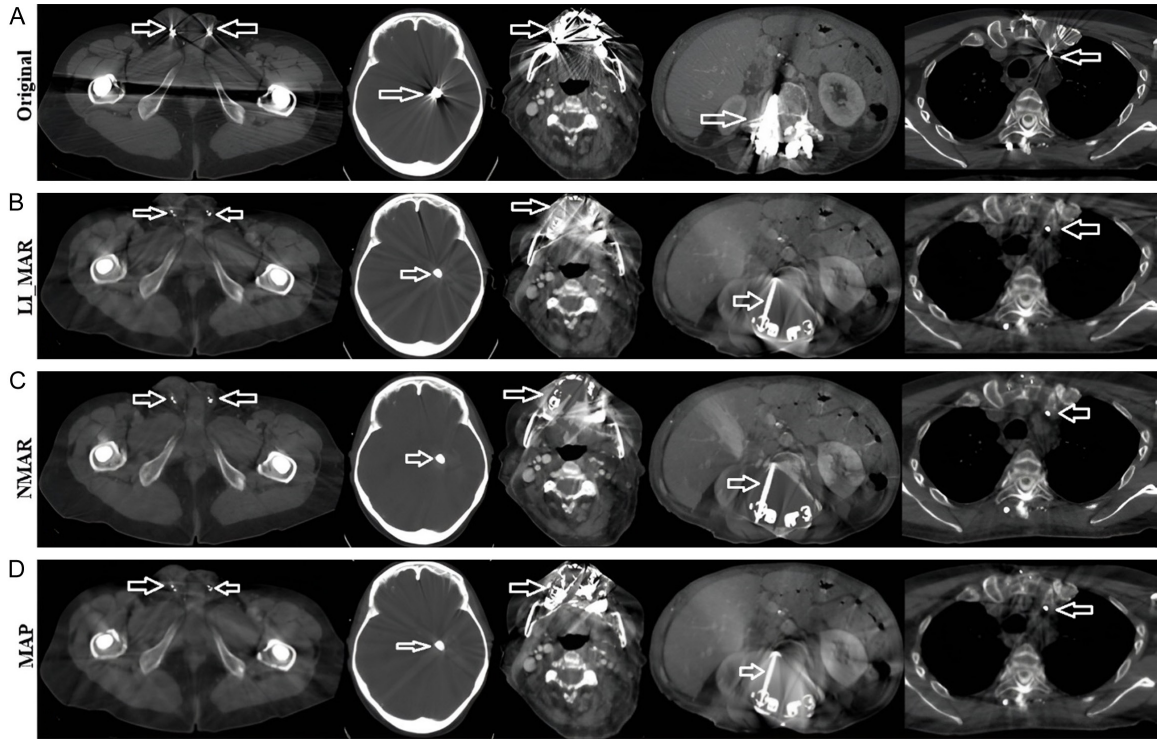

Figure 1. Visual comparison of metal artifact reduction (MAR) performance across different algorithms applied to CT images with metallic implants. Each row corresponds to a different MAR method and each column shows a different anatomical region affected by metallic implants: (from left to right) pelvis, brain, head and neck, abdomen, and chest. A. Original (uncorrected): prominent streaking artifacts and distortions are observed due to the presence of high-density metal objects, severely compromising image quality and obscuring anatomical details. B. LI-MAR: reduces some of the major artifacts but introduces new distortions and fails to fully restore soft tissue contrast, especially in the abdominal and brain regions. C. NMAR: the most effective artifact suppression overall, with significantly improved anatomical visibility and minimal introduction of secondary artifacts. It preserves structural continuity in soft tissue and bone regions, particularly in the pelvis and chest. D. MAP: offers partial artifact reduction but leaves residual streaks and exhibits some image smoothing, which may obscure fine anatomical details.

metallic components near soft tissue. Due to the low artifact intensity, almost all algorithms performed well on this image, and NMAR and MDT did not introduce additional artifacts. As the size and density of metallic implants increase, the resulting artifacts become more severe, making their removal progressively more challenging.

Figure 2A shows the sinogram of the simulated image, where the bright bands correspond to projections related to the metallic region. **Figure 2B** illustrates the sinogram after correction, where the bright bands are completely removed and continuity is restored in the sinogram. In Given the low contrast of the brain in X-ray CT imaging, a metal-free image is expected to exhibit a flat line profile. Comparing the line profiles of images reconstructed using different algorithms, it is observed that NMAR produces the flattest output relative to the other methods. Therefore, the NMAR algorithm demonstrates superior performance in recovering corrupted brain tissue in CT images.

Discussion

The data presents the quantitative evaluation of the MAR algorithms using the normalized root-mean-square error (NRMSE) calculated on the simulated image (**Figure 1**), along with the processing time of each algorithm. Based on the NRMSE values, the NMAR algorithm has the lowest error (NRMSE = 0.175) among all the algorithms, indicating the best overall performance. Another important parameter is the processing time. The LI-MAR algorithm is the fastest algorithm; however, qualitative and quantitative evaluations of its output images indicate lower image quality. In contrast, the NMAR algorithm offers balanced performance, with an NRMSE of 0.175 and a processing time

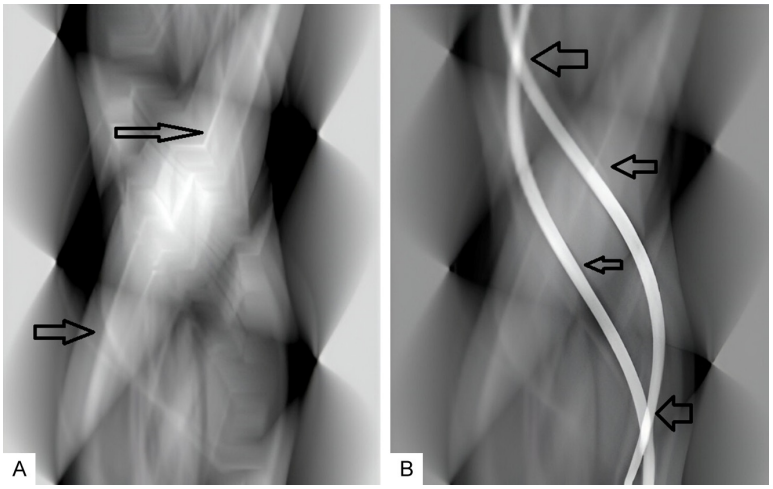

Figure 2. Before and after correction of Sinogram. (A) The sinogram of the simulated image before applying MAR methods is shown. The very bright and saturated bands, seen as vertical or diagonal lines, represent the paths of the rays that have passed through the metal region. The presence of these saturated areas causes severe discontinuities in the sinogram pattern and creates irregular dark and light areas around them. These irregular patterns indicate distortion of the projection data and lead to stretched artifacts and false fills in the reconstructed image. (B) The sinogram is shown after applying the artifact correction method. The bright bands associated with metal have either been completely eliminated or their intensity has been significantly reduced. In contrast to view (A), the sinogram patterns in this image are more continuous, and the intensity lines are visible with a natural slope and no breaks. The overall structure of the sinogram has become smoother and more uniform, and areas that were previously distorted due to metal saturation have now been restored.

of 12.49 seconds, which represents the best balance between accuracy and efficiency among the evaluated MAR algorithms.

This study systematically evaluated five common metal artifact reduction (MAR) algorithms, including LI-MAR, NMAR, MDT, MAP, and OMAR, using clinical and simulated CT images. The results show that while all algorithms are capable of reducing metal artifacts to some extent, the NMAR algorithm consistently outperforms other methods in terms of artifact suppression and accurate recovery of corrupted projections. The NMAR algorithm not only minimizes secondary artifacts but also preserves the structural integrity of anatomical regions, especially in brain imaging [22]. The findings also show that the severity and density of metal implants significantly affect the performance of MAR algorithms, with larger and denser implants posing greater challenges. While the LI-MAR algorithm offers faster processing, it reduces image quality, whereas NMAR achieves the best balance between accuracy and computational efficiency [23].

Future improvements could include the use of advanced segmentation techniques, higher-order interpolation methods, and GPU-accelerated processing to increase both accuracy and speed. Overall, the NMAR algorithm shows great potential for clinical application, providing reliable image correction and supporting accurate detection in CT imaging with the presence of metallic implants [24].

The results of this study are also consistent with the findings of several previous studies; for example, some studies have reported that NMAR performs better than linear re-filling-based methods in reducing severe artifacts caused by dense implants and usually provides a more uniform intensity profile [18]. It has also been noted in other research that LI-MAR and OMAR methods perform acceptable in images with mild artifacts, but in the presence of large implants, they produce secondary artifacts [23]. This was also observed in the results of this study. Other comparative studies have also shown that MDT helps preserve textural details in low-contrast scenarios (such as the brain region) which was confirmed in the head coil images in this study [18, 20].

Overall, the agreement between the present findings and existing reports indicates that the severity and type of artifact is the determining factor in choosing the appropriate MAR method and no algorithm has the same performance in all conditions.

Conclusion

This study shows that the NMAR algorithm is the best MAR algorithm and offers a good balance between accuracy and efficiency. Although the LI-MAR algorithm processes images faster, its quality is not as good as NMAR. The performance of all algorithms depends on the size and density of the implant, highlighting the need for flexible methods. Future improvements should aim to increase accuracy and

speed to make these algorithms more applicable in complex imaging situations.

Disclosure of conflict of interest

None.

Address correspondence to: Hossein Mohammadi, School of Medicine, Isfahan University of Medical Science, Hezar Jarib Street, Isfahan 8174673461, Iran. Tel: +98-9138102548; Fax: +98-9137294009; E-mail: drhossein.mohammadi93@gmail.com

References

[1] Fleischmann D, Chin AS, Molvin L, Wang J and Hallett R. Computed tomography angiography: a review and technical update. Radiol Clin North Am 2016; 54: 1-12.

[2] Rafieezadeh D, Sabeti G, Khalaji A and Mohammadi H. Advances in nanotechnology for targeted drug delivery in neurodegenerative diseases. Am J Neurodegener Dis 2025; 14: 51-57.

[3] Bohner L, Meier N, Gremse F, Tortamano P, Kleinheinz J and Hanisch M. Magnetic resonance imaging artifacts produced by dental implants with different geometries. Dentomaxillofac Radiol 2020; 49: 20200121.

[4] Zaffino P, Marzullo A, Moccia S, Calimeri F, De Momi E, Bertucci B, Arcuri PP and Spadea MF. An open-source COVID-19 CT dataset with automatic lung tissue classification for radiomics. Bioengineering (Basel) 2021; 8: 26.

[5] Rio E, Mornex F, Maingon P, Peiffert D and Parent L. Hepatic tumours and radiotherapy. Cancer Radiother 2022; 26: 266-271.

[6] Liang K, Zhang L, Yang H, Yang Y, Chen Z and Xing Y. Metal artifact reduction for practical dental computed tomography by improving interpolation-based reconstruction with deep learning. Med Phys 2019; 46: e823-e834.

[7] Zhu M, Zhu Q, Song Y, Guo Y, Zeng D, Bian Z, Wang Y and Ma J. Physics-informed sinogram completion for metal artifact reduction in CT imaging. Phys Med Biol 2023; 68: [Epub ahead of print].

[8] Jagoda P, Schmitz D, Wagenpfeil S, Bücker A and Minko P. Comparison of metal artifact reduction in dual- and single-source CT: a vertebral phantom study. AJR Am J Roentgenol 2018; 211: 1298-1305.

[9] Laukamp KR, Zopfs D, Lennartz S, Pennig L, Maintz D, Borggrefe J and Große Hokamp N. Metal artifacts in patients with large dental implants and bridges: combination of metal artifact reduction algorithms and virtual monoenergetic images provides an approach to handle even strongest artifacts. Eur Radiol 2019; 29: 4228-4238.

[10] Kim C, Pua R, Lee CH, Choi DI, Cho B, Lee SW, Cho S and Kwak J. An additional tilted-scan-based CT metal-artifact-reduction method for radiation therapy planning. J Appl Clin Med Phys 2019; 20: 237-249.

[11] Hegazy MAA, Eldib ME, Hernandez D, Cho MH, Cho MH and Lee SY. Dual-energy-based metal segmentation for metal artifact reduction in dental computed tomography. Med Phys 2018; 45: 714-724.

[12] Meyer E, Raupach R, Lell M, Schmidt B and Kachelriess M. Normalized metal artifact reduction (NMAR) in computed tomography. Med Phys 2010; 37: 5482-5493.

[13] Steiding C, Kolditz D and Kalender WA. A quality assurance framework for the fully automated and objective evaluation of image quality in cone-beam computed tomography. Med Phys 2014; 41: 031901.

[14] Humphries T and Wang BJ. Superiorized method for metal artifact reduction. Med Phys 2020; 47: 3984-3995.

[15] Richtsmeier D, O'Connell J, Rodesch PA, Iniewski K and Bazalova-Carter M. Metal artifact correction in photon-counting detector computed tomography: metal trace replacement using high-energy data. Med Phys 2023; 50: 380-396.

[16] Khalaji A, Riahi F, Rafieezadeh D, Khademi F, Fesharaki S and Joni SS. Artificial intelligence in automated detection of lung nodules: a narrative review. Int J Physiol Pathophysiol Pharmacol 2025; 17: 45-51.

[17] Boas FE and Fleischmann D. Evaluation of two iterative techniques for reducing metal artifacts in computed tomography. Radiology 2011; 259: 894-902.

[18] Woo H, Chai JW, Choi YH and Jin KN. Metal artifact reduction for orthopedic prosthesis in lower extremity CT venography: evaluation of image quality and vessel conspicuity. Cardiovasc Intervent Radiol 2019; 42: 1619-1626.

[19] Peschke E, Ulloa P, Jansen O and Hoevener JB. Metallic implants in MRI - hazards and imaging artifacts. Rofo 2021; 193: 1285-1293.

[20] Kim DS and Kim E. Noise power spectrum of the fixed pattern noise in digital radiography detectors. Med Phys 2016; 43: 2765-2773.

[21] Maughan NM, Garcia-Ramirez J, Arpidone M, Swallen A, Laforest R, Goddu SM, Parikh PJ and Zoberi JE. Validation of post-treatment PET-based dosimetry software for hepatic radioembolization of Yttrium-90 microspheres. Med Phys 2019; 46: 2394-2402.

[22] Morioka Y, Ichikawa K and Kawashima H. Quality improvement of images with metal arti-

fact reduction using a noise recovery technique in computed tomography. Phys Eng Sci Med 2024; 47: 169-180.

[23] Lustermans D, Fonseca GP, Taasti VT, van de Schoot A, Petit S, van Elmpt W and Verhaegen F. Image quality evaluation of a new high-performance ring-gantry cone-beam computed tomography imager. Phys Med Biol 2024; 69 [Epub ahead of print].

[24] Meyer E, Raupach R, Lell M, Schmidt B and Kachelrieß M. Frequency split metal artifact reduction (FSMAR) in computed tomography. Med Phys 2012; 39: 1904-1916.